View metadata, citation and similar papers at core.ac.uk
brought to you by CORE
provided by Universiti Malaysia Kelantan Intitutional Repository

J. Trop. Resour. Sustain. Sci. 5 (2017): 1-8

Journal of Tropical Resources and Sustainable Science

journal homepage: jtrss.org

Effectiveness of 2-D Resistivity Survey to Identify Lineament (Fault) from Photolineament Interpretation – Case Study at Kampung Dato' Mufti, Ampang, Selangor

Hamzah Hussin[1, 2,*], Mohd Hariri Ariffin[2], Mohd Amir Asyraf Sulaiman[2], Nurhazren Fauzi[1]

[1]Faculty of Earth Science, Universiti Malaysia Kelantan, Jeli Campus, Jeli, Kelantan, Malaysia
[2]Faculty of Science & Technology, Universiti Kebangsaan Malaysia, Bangi, Selangor, Malaysia

Received 18 March 2015
Accepted 20 August 2015
Online 1 June 2017

Keywords:
Lineament, photolineament, electrical resistivity, Wenner configuration.

⊠*Corresponding author:
Hamzah Hussin,
Faculty of Earth Science,
Universiti Malaysia Kelantan,
Jeli Campus, Jeli, Kelantan,
Malaysia.
Faculty of Science &
Technology, Universiti
Kebangsaan Malaysia, Bangi,
Selangor, Malaysia.
Email: hamzah.h@umk.edu.my

Abstract

Lineaments play an important role in the stability of structures such as slopes, foundations, dams and buildings. Identification of the presence of lineament is important especially at planning and construction stage to enable mitigation measures/controls can selected earlier. The combined techniques of satellite image downloaded from Google Earth interpretation and electrical resistivity survey can assist in the identification and verification process of lineament structures. In this study, interpretation of lineament was done using satellite images Google Earth in the laboratory. Orientation and position of every lineament was determined accurately in the field. Electrical resistivity survey was conducted using Wanner configuration that cross the lineament in the field. The electrical resistivity results showed the presence of lineament structural in the pseudo section and prove the effectiveness of combination of both techniques to detect and confirm the presence of structural lineament.

© 2017 UMK Publisher. All rights reserved.

1. Introduction

Lineament mapping was used before in other geological applications and the first usage of the term lineament in geology is probably by Hobbs who defined lineaments as significant lines of landscape caused by joints and faults, revealing the architecture of the rock basement (Hobbs, 1904; Hobbs, 1912). Lineaments are lines on satellite imageries that are expression of folds, fractures, or faults in the subsurface (Sabins, 2000). These features are mappable at various scales, from local to continental.

Lineaments are considered to be naturally occurring, mappable linear topographic features on Earth's surface that may be formed by fractures in Earth's crust, which can be joints, faults, or shear zones (Boyer & McQueen, 1964; O'leary et al., 1976; Sabins, 2000). Lineament or straightness in the earth's surface can be obtained using rocks topographic maps, satellite images and aerial photographs (Hamzah & Tajul Anuar, 2011; Kim, 1979; Norman & Partridge, 1978; Tjia, 1971; Tjia, 1972). Every method has the advantages and disadvantages of its own.

Identification of lineament is vital in various field such as construction, oil and gas exploration, mining, ground water exploration and landform studies (Marghany, 2012; Omosanya et. al, 2012; Rida, 2012). One of the methods to emphases in this paper is the used of Google Earth Pro to identify major lineament. Google Earth Pro is free and the easiest way to get satellite image data. Google Earth Pro is proven to be a highly effective tool for gathering lineament orientation and spatial distribution data (Lageson et al., 2012; Rana et al, 2016). To verify lineament interpretation, resistivity survey was conducted across lineament orientation.

2D geoelectrical resistivity imaging or tomography surveys is new development in recent years to map areas with moderately complex geology (Griffiths & Barker, 1993) and can contribute a lot to the subsurface study of fractured bedrocks by helping to identify the fractured and or weak zones (Arifin et al., 2016). The resistivity of the subsurface material can be measured by injecting a small current into the ground through two electrodes and the resulting voltage on the ground surface is measured at two potential electrodes. By varying the spacing between the electrodes, as well as the location of the electrodes, a 2-D electrical resistivity image of the subsurface can be obtained.

eISSN Number: 2462-2389 © 2017 UMK Publisher. All rights reserved.

2. Materials and Methods

2.1. Study Area

The study was conducted at Kg Dato' Mufti, Ampang, Selangor at coordinate of 3°8'52.86" N and 101°46'56.97"E. Total area that was covered in this study is 0.50km^2. Figure 1 shows the location of study area.

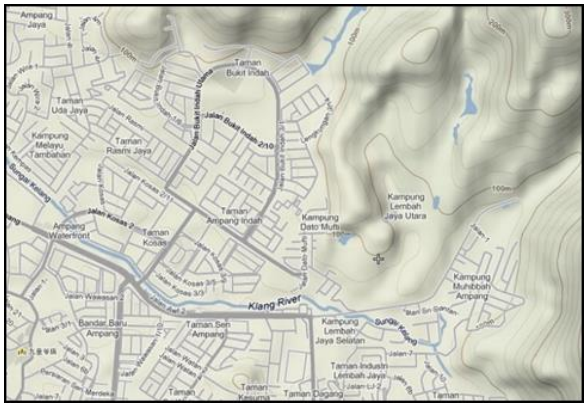

Figure 1: Location of site is marked by blue box located in Ampang District, Selangor

2.2. Regional Geological Setting Sample

Regional geology of the Kuala Lumpur and part of Selangor (or Kelang Basin) is underlined by Lower to Upper Paleozoic metamorphic and metasedimentary rock sequences, which were intruded by Late Triassic granite and the associated late-phase intrusions (Gobbett, 1964). On a regional scale, the Kuala Lumpur area (including the study area) is situated in the central part of the Western Belt of the Peninsular Malaysia. It is underlined by strongly folded and regionally metamorphosed clastic and calcareous Lower Paleozoic rocks and a sequence of folded Upper Paleozoic clastic metasediments.

The oldest rocks in this region are represented by regional metamorphic rocks; known as Hawthornden Schist and Dinding Schist Formations (Yin, 1976). The Hawthornden Schists are made up of predominantly graphitic schist and quartz-mica schist. The Dinding Schists are made up of predominantly of quartz-mica schist derived from rhyolitic volcanic. The schists are characterized by a well-developed schistosity that had been folded and crenulated. Overlying unconformably the older metamorphic rocks is the Kuala Lumpur Limestone, which is made up of hard and very strong light grey to dark grey limestone and marble. They commonly occur as the bedrock to the unconsolidated alluvial deposits in the low lying areas of Kuala Lumpur, Serdang, Sungai Besi, and Gombak.

The Kenny Hill Formation lies unconformably over the Kuala Lumpur Limestone. It is made up of an alternating sandstone and shale sequence that exhibit low grade regional metamorphism. The Kenny Hill Formation has been variously open to tightly fold in a major N-S synformal structure. All the strata have been deformed by predominantly strike-slip faulting. The faults strike generally NW, WNW, N and NE. Figure 2 shows the simplified geological map of Kuala Lumpur and parts of Selangor region.

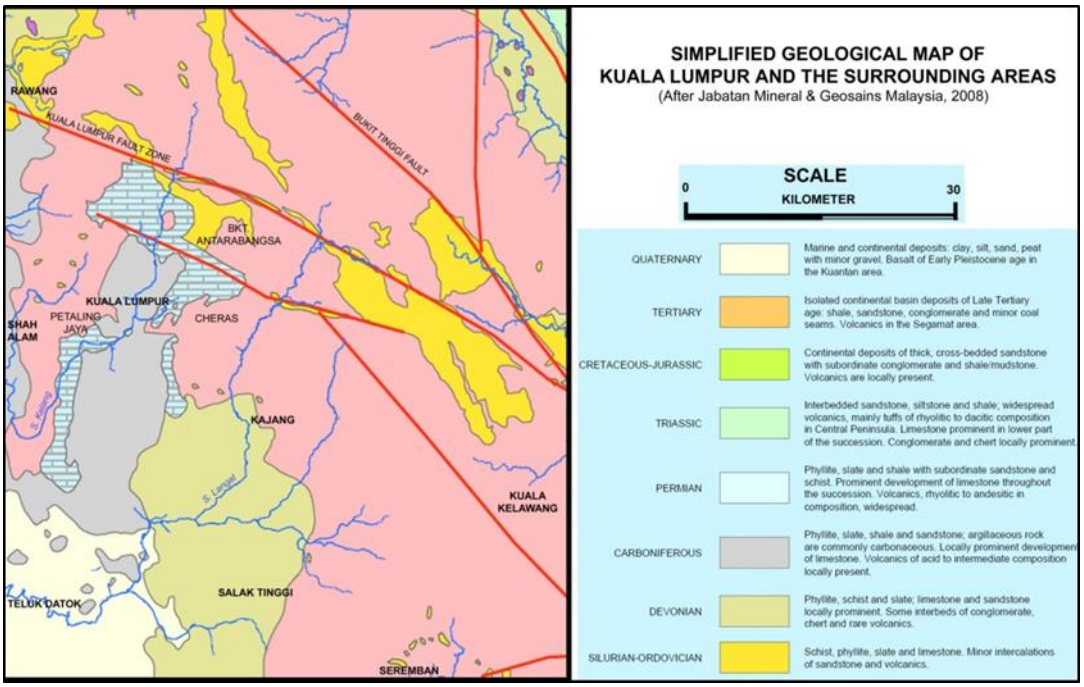

Figure 2: Simplified geological map of part of Selangor and Wilayah Persekutuan Kuala Lumpur (Singh, 1985)

eISSN Number: 2462-2389 © 2017
UMK Publisher. All rights reserved.

2.3. Site Geology and Site Condition

The geology of the site consisting essentially of granite. The granite is light grey, medium grained size (Figure 3). Granitic rock consist quartz, feldspar and plagioclase mineral which measures up to 0.5-1.0 cm in size. Biotite presents as minor mineralogy constituents. This granite rock mass had been excavated for the use as aggregate on the west of study area as shown in Figure 4.

Figure 3: Close-up view of fresh, medium-grained granite

Figure 4: View of granite slope face of ex-quarry on the west of study area which have been excavate for aggregate

Figure 5: Heavy densities of vegetation around study area have cause difficulty for resistivity survey to be done

Resistivity lines survey are located at the ridge which orientated in north-south direction with the average slope gradient of 60°. The highest point of height is 135m from ground level. The length of the ridge is approximately 500m with covered with shrubs and small trees including on top of the slope (Figure 5). Pieces of rock fragment in various sizes from pebble to cobble can be observed on the north and top of the slope.

2.4. Weathering

In this research, degree of weathering for the rock masses is described using the classification scheme by International Society for Rock (ISRM), 1981. The studied area is varies in weathering grade from fresh (grade I) to slightly and moderately (grade II-III) and highly to completely weathered (grade IV-V). The fresh and slightly weathered rocks are generally exposed at the east flank of the ridge, while the moderately (Figure 6) and highly weathered rock masses are exposed at the center and south flank of the ridge respectively. Grade VI or residual soils formed the overburden at the top of the slope.

The fresh to slightly and moderately weathered granite rock material are generally very strong to extremely strong rock. As the weathering grade increase, the strength of the rock material decreases due to alteration and decomposition of its constituent materials. Highly weathered granite material generally became medium strong rock, and the completely weathered granite may become weak or very weak rock or behaving more towards soils (Figure 7).

Figure 6: Moderately weathered granite exposed at the top of study area

eISSN Number: 2462-2389 © 2017 UMK Publisher. All rights reserved.

Figure 7: Close-up view of completely weathered granite rock mass shown

2.5. Photolineament Study

Photolineaments study was carried out to determine regional lineament at site project and surrounding area. The main focus of the API is to identify the major structural features of the study area, notably the negative lineament to be evidence for an interpretation from resistivity survey. The result from photolineament interpretation is shown in Figure 8. The lineaments are shown as yellow lines in this figure. Result of the photolineament study suggests that the area is dissected by at least 3 sets of lineament, mainly strike in NW-SE, NE-SW and W-E directions. Most dominant lineaments are oriented in NW-SE and NE-SW direction.

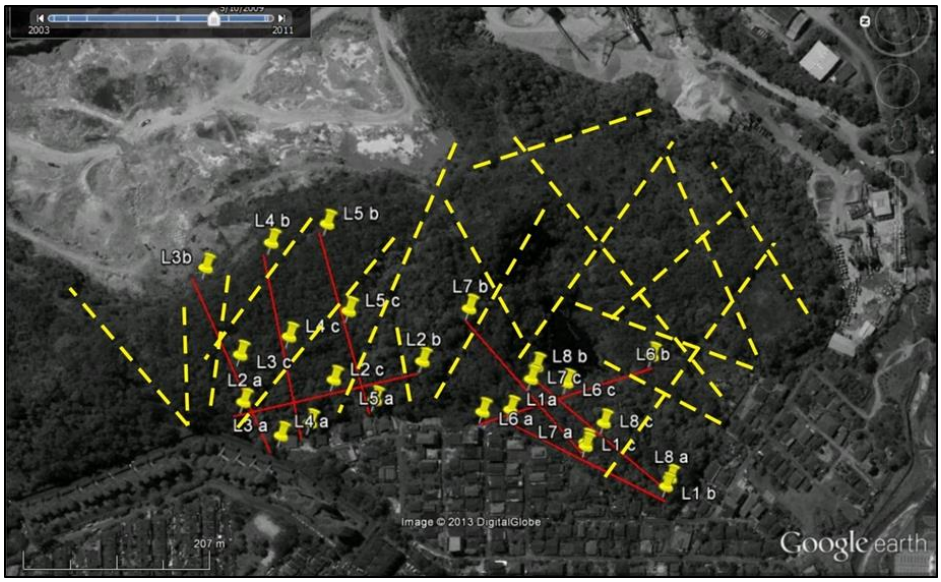

Figure 8: Lineament interpretation (yellow dash) from satellite image at site project and its overlay with electrical resistivity survey line (solid red line)

2.6. Resistivity Survey

The 2-D electrical imaging survey was carried out with a SAS4000 resistivity meter and ABEM LUND ES464 electrode selector system (Figure 9).

Figure 9: The set of ABEM SAS1000 resistivity meter and ABEM LUND ES464 electrode selector system

This system is connected to 41 steel electrodes which lay out on a straight line with a constant spacing via a multicore cable. A microcomputer connected to the resistivity unit then automatically selects the four active electrodes used for each measurement. The Wenner equal spacing electrode array was used for this survey. For more details about the survey and interpretation method, please refer to the papers by Griffiths & Barker (1993) and Loke & Barker (1996).

The resistivity of the subsurface materials depends on several factors such as the nature of the solid matrix and its porosity, as well as the type of fluids (normally water or air) which fill the pores of the rock or soil. In general, rock and dry soil have high resistivity of several hundred or thousands ohm-meter. Fractured rock saturated with water has relatively low resistivity values of generally below 1000 ohm-m.

A total of eight lines of resistivity survey had been done. Total lengths for each resistivity survey lines are 200m and its electrode spacing is 5m (Figure 10). The measured resistivity survey data were interpreted using RES2DINV inversion software.

eISSN Number: 2462-2389 © 2017
UMK Publisher. All rights reserved.

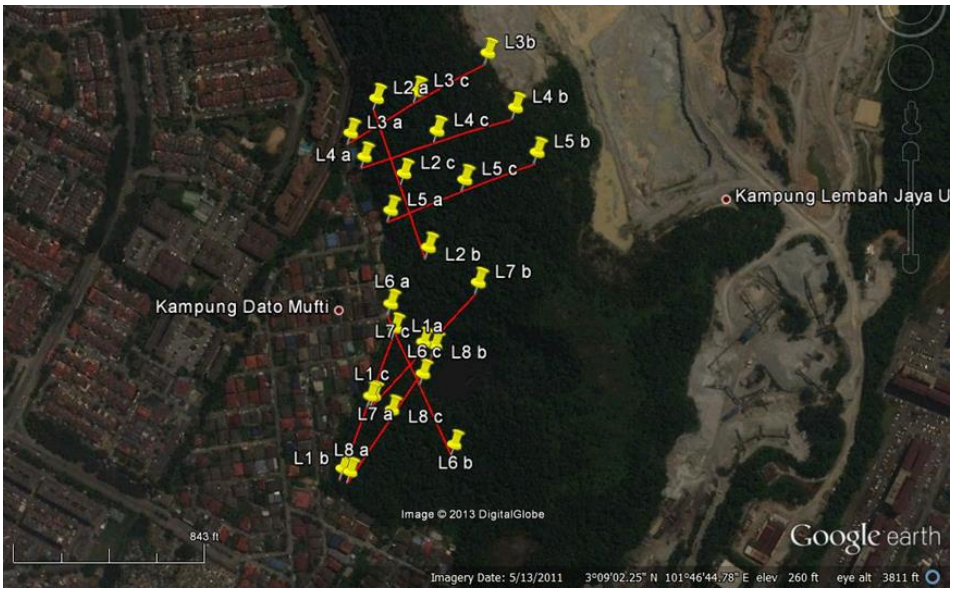

Figure 10: Location for 8 lines of resistivity survey which have been done

3. Results and Discussion

3.1. Resistivity Survey Line 1 (DM 1)

The total profile length of resistivity line DM 1 is 200m with 5m electrode spacing. This line is north-south in direction (Figure 11). The resistivity values of the sub-surface profile ranges between 35.8 Ωm to 12,662 Ωm. Four different profiles can be clearly seen in interpretation are bedrock, overburden soil, highly weathered rock and water saturated zone. Overburden soil is more dominant on the left of survey line while bedrock is dominant on other site. The thickness of the overburden layer is approximately 20m. The bedrock is generally shown by the highest resistivity values compare to others. At a depth of 10m, low resistivity area can be found in an interpretation data which are suspected as water containing zone.

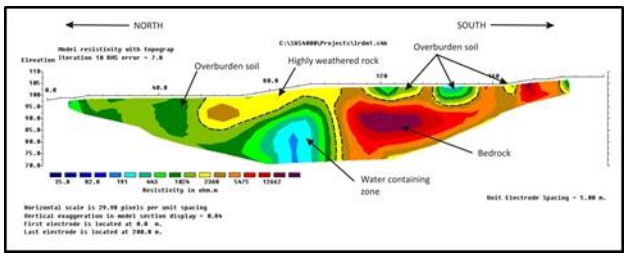

Figure 11: Resistivity interpretations for line DM 1

3.2. Resistivity Survey Line 2 (DM 2)

Resistivity line DM 2 was conducted along north-south profile (Figure 12). The total spread length is 200m with 5m electrode spacing. Two different anomalies are clearly shown in interpretation image which is bedrock and overburden soil. Bedrock material can be found on both end of survey line while overburden soil is located in centre survey line. This abnormal anomaly is believed to be associated with fault zone as be interpreted from photolineament study. Resistivity value for overburden soil is ranging from 143 Ωm to 227 Ωm and for bedrock material, its value is more than 573 Ωm.

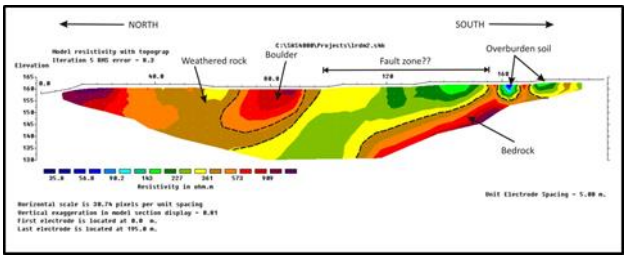

Figure 12: Resistivity interpretation for line DM 2

3.3. Resistivity Survey Line 3 (DM 3)

The total profile length of resistivity line DM 3 is 200m with 5m electrode spacing. This line is southwest-northeast in direction (Figure 13). From resistivity interpretation, sharp contact between bedrock and overburden soil is indicates the presence of fault zone. This major fault zone is obtained from the traced lineament in photolineament study. Resistivity value for bedrock is ranging from 881 Ωm to 1503 Ωm. Bedrock is dominant on the southwest of survey line. On the top of bedrock, a lot of granite boulders can be found at this survey line. These huge granite boulders were believed as dumping from ex-quarry during its operation. At the depth of 10m from surface, water containing zone was detected.

eISSN Number: 2462-2389 © 2017
UMK Publisher. All rights reserved.

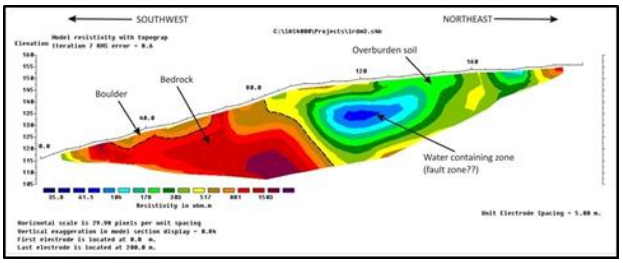

Figure 13: Resistivity interpretation for line DM 3

3.4. Resistivity Survey Line 4 (DM 4)

Resistivity line DM 4 (Figure 14) was conducted along southwest-northeast. The total profile length is 200m with 5m electrode spacing. This line is parallel to line DM 3. Water containing zone was identified at the distance of 55m from the first electrode. This zone has a low resistivity value (<150 Ωm) and was believed is to be associated with lineament features. Granite bedrock is detected from electrode first until electrode 12th. The resistivity value is more than 2618 Ωm. Granite bedrock can be found at the toe of the ridge at the depth of 8m from surface.

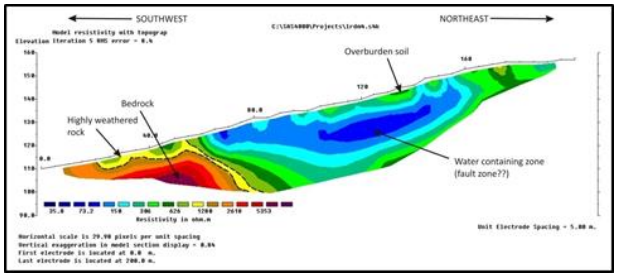

Figure 14: Resistivity interpretation for line DM 4

3.5. Resistivity Survey Line 5 (DM 5)

The resistivity line DM 5 is oriented along northeast-southwest direction crossing the DM 2 line. The resistivity survey was conducted using 5m electrode spacing configuration which produced 200 meter length of 2-D resistivity profile. . The resistivity interpretation along DM 5 is shown in Figure 15. The lowest resistivity value is <35.8 Ωm and the highest value is >2466 Ωm. This resistivity survey line profile is almost same as DM 3 and DM 4 as it clearly shows two different anomalies of electrical resistivity. The presence of fault zone on the northeast survey line had affected the resistivity value. A minor fault zone can also be detected at an 8th electrode. Bedrock and granite boulder have highest resistivity value which is >1347 Ωm.

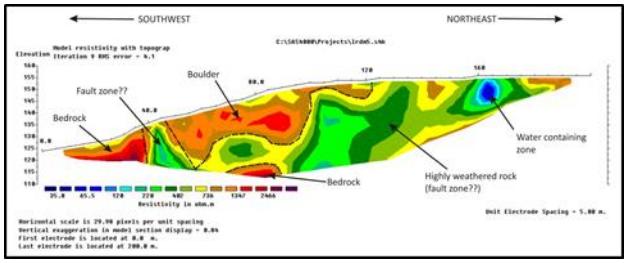

Figure 15: Resistivity interpretation for line DM 5

3.6. Resistivity Survey Line 6 (DM 6)

The total profile length of resistivity line DM 6 is 200m with 5m electrode spacing. This line is northwest-southeast in direction (Figure 16). The resistivity values of the sub-surface profile ranges between <35.8 Ωm to >4224 Ωm. A fault zone is identified from this interpretation located at center of survey line. Granite bedrock and boulder are dominant in this interpretation.

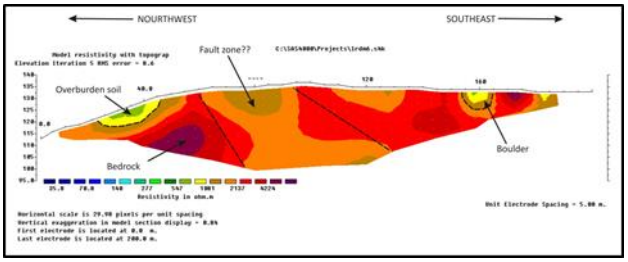

Figure 16: Resistivity interpretation for line DM 6

3.7. Resistivity Survey Line 7 (DM 7)

Resistivity line DM 7 was conducted along southwest-northeast profile with 200m total length and 5m electrode spacing. This line crossed DM 6. Figure 17 shows resistivity interpretation for DM 7. Based on the resistivity profile, two zone have been detected which is bedrock and highly weathered rock. Highly weathered rock is located on southwest of survey line while granite bedrock is dominant on northeast of study line.

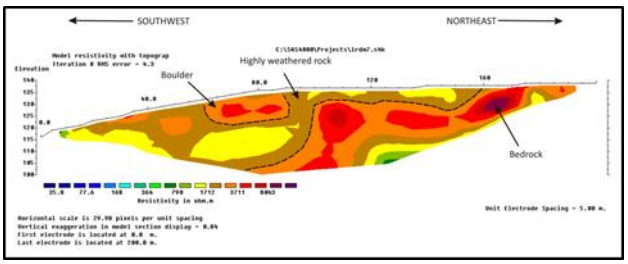

Figure 17: Resistivity interpretation for line DM 7

3.8. Resistivity Survey Line 8 (DM 8)

The total profile length of resistivity line DM 8 is 200m with 5m electrode spacing. This line is southwest-northeast in direction. The resistivity interpretation along DM 8 is shown in Figure 18. From resistivity interpretation, two fault zones are interpreted based on the sudden change in resistivity anomaly. This major fault zone was confirmed from the traced lineament in photolineament study. Resistivity value for bedrock is > 3973 Ωm. Bedrock is dominant on the center of survey line. At the depth of 20m from surface, water saturated zone was detected. On the toe of survey line, overburden soil is more dominant and its thickness can reach 15m depth.

eISSN Number: 2462-2389 © 2017
UMK Publisher. All rights reserved.

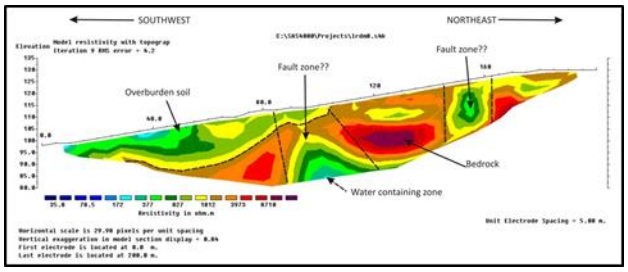

Figure 18: Resistivity interpretation for line DM 8

4. Conclusion

A total of eight resistivity lines have been conducted to covers all of the study area. Summary of findings is shown in Figure 19. These surveys provide important information in the study area via resistivity mapping. The survey is significant because it can be used to identify weak zone and useful to minimize hazards associated with the unstable area. Based on this investigation, there is a significant change of resistivity value for each line of survey line because of the presence of major fault zone especially on the north of study area. This interpretation is supported by photolineament study which shows orientation and density of major lineament from study area and its connection with resistivity interpretation.

From resistivity data interpretation, three major zones can be detected which are bedrock, overburden soil and water containing zone. Depth of bedrock varies from a survey line to another survey line. Depth of fresh bedrock can be achieved at the depth of 10-15m from surface. As a result from weathering process, various thickness of overburden soil can be found at study area. The thickness varies from 1m to 10m. As a suggestion, drilling method can be used to reconfirm the suspected area using continuous undisturbed sample. The sample/soil profile must be collected and recorded for a better interpretation finding.

Interpretation from resistivity data shown good correlation with lineament mapping. This has proof suitability of resistivity survey to support lineament interpretation from aerial photo of satellite image.

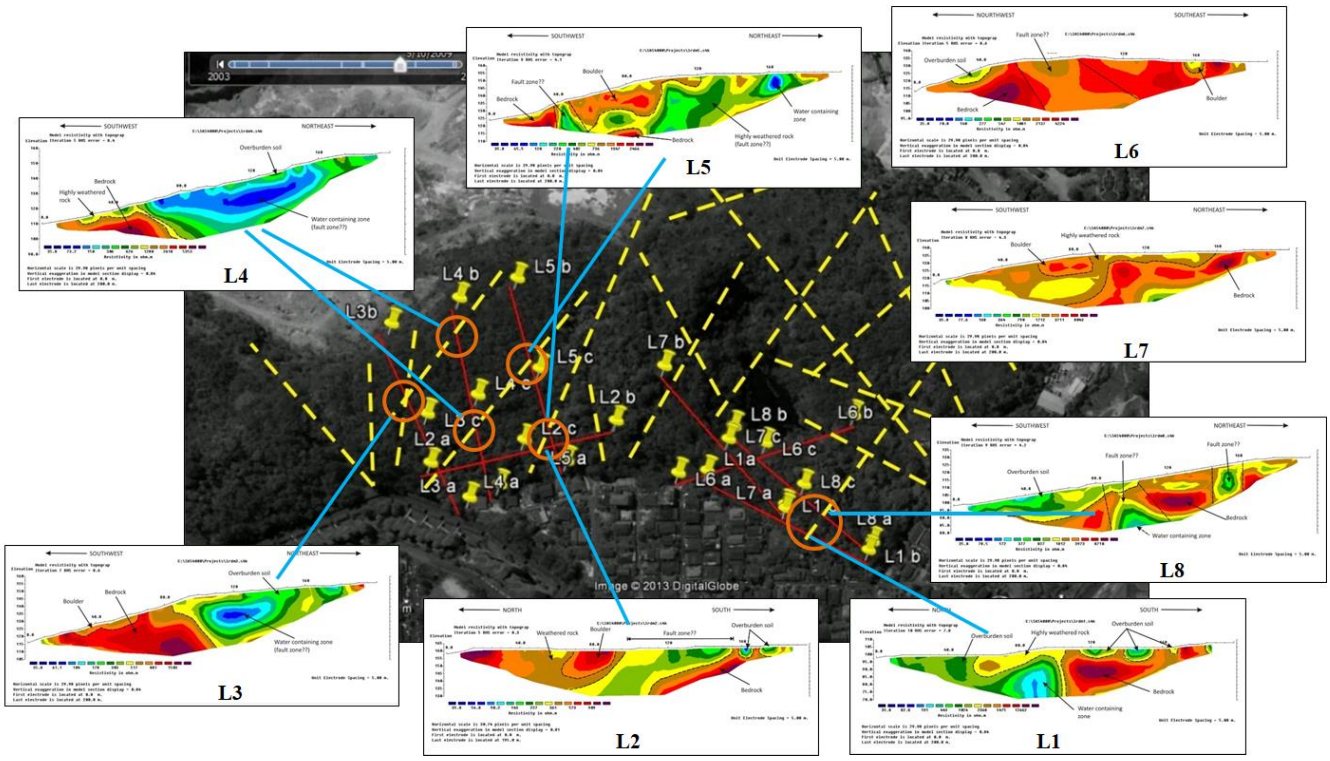

Figure 19: Summary of resistivity and lineament analysis

Acknowledgement

The authors would like to thank GeoTechnology Resources Sdn Bhd (GTR) for give an approval to conduct this research at their site area.

References

Arifin, M. H., Jamaluddin, T. A., Husin, H., Ismail, A., Abbas, A. A., Nordin, M. N. M., … Othman, N. A. (2016). Comparison of geological mapping with electrical resistivity and ground penetration radar methods for rock fractured system study. Chiang Mai Journal of Science, 43(6Special Issue 2), 1346–1357.

Bieniawski, Z. . (1975). Case studies: Prediction of rock mass behavior by the geomechanics classification. In Proceedings of 2nd Australia–New Zealand Conference Geomechanics, Brisbane. (pp. 36–41).

Boyer, R., & McQueen, J. (1964). Comparison of mapped rock fractures and airphoto linear features. Photogrammetric Engineering and Remote Sensing, 30(4), 630–635.

Gobbett, D. J. (1964). The lower palaeozoic rocks of Kuala Lumpur, Malaysia. Fed Mus J, 9, 67–79.

eISSN Number: 2462-2389 © 2017
UMK Publisher. All rights reserved.

Griffiths, D. H., & Barker, R. D. (1993). Two-dimensional resistivity imaging and modelling in areas of complex geology. Journal of Applied Geophysics, 29(3), 211–226.

Hamzah, H. & Tajul Anuar, J. (2011). Kajian fotograf udara untuk geologi kejuruteraan cerun di kawasan Bukit Chendering, Kuala Terengganu. In National Geoscience Conference (p. 39).

Hobbs, W. H. (1904). Lineaments of the Atlantic border region. Geological Society of America Bulletin, 15(1), 483–506.

Hobbs, W. H. (1912). Earth features and their meaning: an introduction to geology for the student and the general reader. The Macmillan Company.

International Society For Rock (ISRM). (1981). Rock characterization, testing & monitoring: ISRM suggested methods. (E. T. Brown, Ed.). Pergamon Press.

Kim, S.-K. (1979). Analyses of Lineaments Extracted From LANDSAT Images of the Korean Peninsula. The Journal of Earth Sciences, 26, 49–74.

Lageson, D. R., Larsen, M. C., Lynn, H. B., & Treadway, W. A. (2012). Applications of Google Earth Pro to fracture and fault studies of Laramide anticlines in the Rocky Mountain foreland. Geological Society of America Special Papers, 492, 209–220.

Loke, M. H., & Barker, R. D. (1996). Rapid least-squares inversion of apparent resistivity pseudosections by a quasi-Newton method. Geophysical Prospecting, 44(1), 131–152.

Marghany, M. (2012). Fuzzy B-spline algorithm for 3-D lineament reconstruction. International Journal of Physical Sciences, 7(15), 2294–2301.

Norman, J. W., & Partridge, T. C. (1978). Fracture analysis in the determination of subunconformity structure: A photogeological study. Journal of Petroleum Geology, 1(1), 43–63.

O'leary, D. W., Friedman, J. D., & Pohn, H. A. (1976). Lineament, linear, lineation: some proposed new standards for old terms. Geological Society of America Bulletin, 87(10), 1463–1469.

Omosanya, K. O., Akinbodewa, A. E., & Mosuro, G. O. (2012). Integrated mapping of lineaments in Ago-Iwoye SE, SW Nigeria. International Journal of Science and Technology, 1(2), 68–79.

Rana, N., Chakravarthy, C. P., Nair, R., & Kannan, L. G. (2016). Identification of lineaments using Google tools. In Recent Advances in Rock Engineering (RARE 2016) (pp. 124–132). Atlantis Press.

Rida, A.-A. (2012). The Use of GIS and Google Earth for Preliminary Site Selection of Groundwater Recharge in the Azraq Oasis Area—Jordan. Journal of Water Resource and Protection, 4, 395–399.

Sabins, F. F. (2000). Remote Sensing – Principles and Interpretation. New York: W.H.Freeman and Company.

Sabins, F. F. (2000). Remote Sensing – Principles and Interpretation. New York: W.H.Freeman and Company.

Singh, D. S. (1985). Geological map of West Malaysia. 8th Edition. Geological Survey of Malaysia.

Tjia, H. . (1971). Lineament pattern of Penang Island, West Malaysia. The Journal of Tropical Geography, 1, 24–29.

Tjia, H. D. (1972). Lineamen-lineamen Malaysia Barat. Ilmu Alam, 1, 24–29.

Yin, E.H. (1976). Geological map of Selangor. Diterbitkan oleh Ketua Pengarah, Jabatan Penyiastan Kajibumi Malaysia, Ipoh Semenanjung Malaysia.

eISSN Number: 2462-2389 © 2017
UMK Publisher. All rights reserved.